AIAA JOURNAL
Vol. 43, No. 9, September 2005

Similarity Analysis for Transpired Turbulent Boundary Layers Subjected to External Pressure Gradients

Raúl Bayoán Cal* and Luciano Castillo†
Rensselaer Polytechnic Institute, Troy, New York 12180

The problem of transpired turbulent boundary layers with and without pressure gradient has been studied using similarity analysis of the equations of motion. A blowing parameter has been obtained from the similarity analysis, which includes the imposed vertical velocity at the wall. By using the experimental data from Andersen et al. (Andersen, P. S., Kays, W. M., and Moffat, R. J., "The Turbulent Boundary Layer on a Porous Plate: An Experimental Study of the Fluid Mechanics for Adverse Free-Stream Pressure Gradients," Dept. of Mechanical Engineering, Stanford Univ., Rept. HMT-15, Stanford, CA, May 1972), several notable results were found. First, the mean deficit profiles subjected to suction or blowing in zero pressure gradient and adverse pressure gradient collapse with the freestream velocity, but to different curves depending on the strength of the blowing parameter and the pressure gradient. Second, the dependencies on the blowing parameter, the local Reynolds number, and the strength of pressure gradient are nearly removed from the outer flow when the mean deficit profiles are normalized by the Zagarola/Smits scaling, $U_\infty(\delta_*/\delta)$. Third, the boundary layers subjected to suction or blowing are in equilibrium when the pressure parameter $\Lambda \equiv [\delta/\rho U_\infty^2(\mathrm{d}\delta/\mathrm{d}x)](\mathrm{d}P_\infty/\mathrm{d}x)$ is a constant. Moreover, the value of this constant is directly affected by the blowing parameter, $V_0^+ = [V_0/U_\infty(\mathrm{d}\delta/\mathrm{d}x)]$.

Nomenclature

C_f	=	friction factor
$\mathrm{d}\delta/\mathrm{d}x$	=	boundary-layer growth
f_{op}	=	outer velocity profile (at finite δ^+)
f_{op_∞}	=	asymptotic outer velocity profile in the limit as $\delta^+ \to \infty$
H	=	shape factor, δ_*/θ
R_{so}	=	outer Reynolds stress scale
Re_x	=	Reynolds number based on x
Re_δ	=	Reynolds number based on δ
Re_θ	=	Reynolds number based on θ
U_{so}	=	unknown outer velocity scale
U_∞	=	freestream velocity
$U_\infty - U$	=	mean velocity deficit
$U_\infty\delta_*/\delta$	=	Zagarola/Smits scaling
u_*	=	friction velocity, $\sqrt{(\tau_w/\rho)}$
V_0	=	blowing velocity
V_0^+	=	blowing parameter, $V_0/U_\infty(\mathrm{d}\delta/\mathrm{d}x)$
$\bar{y}$	=	outer similarity length scale, y/δ
β	=	Clauser pressure gradient parameter, $(\delta_*/\rho u_*^2)(\mathrm{d}P_\infty/\mathrm{d}x)$
δ	=	boundary-layer thickness, e.g., δ_{95}
δ_*	=	displacement thickness, $\int_0^\infty (1 - U/U_\infty)\,\mathrm{d}y$
δ^+	=	local Reynolds-number dependence, $\delta u_*/\nu$
θ	=	momentum thickness, $\int_0^\infty (U/U_\infty)(1 - U/U_\infty)\,\mathrm{d}y$
Λ	=	pressure parameter, $[\delta/\rho U_\infty^2(\mathrm{d}\delta/\mathrm{d}x)](\mathrm{d}P_\infty/\mathrm{d}x)$
Λ_β	=	transpired pressure parameter, $(\delta/\rho U_\infty V_0)(\mathrm{d}P_\infty/\mathrm{d}x)$
$*$	=	unknown dependence on upstream conditions

I. Introduction

TRANSPIRED boundary layers have been extensively studied in fluid mechanics because of their industrial applications particularly to flow control. Some of the advantages of using transpiration are retarding separation through the use of suction and increasing the boundary-layer thickness when using blowing. In past studies, this transpiration effect has been denominated by a blowing parameter, which was prescribed by Simpson et al.[1] as

$$B_1 = (\dot{m}''/G')/(C_f/2) \tag{1}$$

and by Andersen et al.[2] as

$$B_2 = V_0 U_\infty/(\tau_w/\rho) \tag{2}$$

By means of nondimensionalization, the blowing parameter in Eq. (1) was defined using the density times the velocity at the wall $\dot{m}'' = \rho_o V_0$, the skin-friction coefficient C_f, and a variable that describes the density times the freestream velocity $G' = (\rho U)_\infty$. Similarly in Eq. (2), a nondimensionalized parameter B_2 was formed using the blowing velocity V_0, the fluid density ρ, the freestream velocity U_∞, and the wall shear stress τ_w. Both research groups performed a series of experiments in which the transpired velocity V_0 was kept constant or it was varied along the streamwise direction x. Their primary concern was to find and analyze the skin-friction coefficient C_f. Furthermore, their analysis was based on the law of the wall for boundary layers with and without pressure gradients.

In 1977, Schetz and Nerney[3] used blowing and surface roughness to illustrate the problem of transpiration in turbulent boundary layers. The blowing velocity was normalized using the friction velocity u_*, thus forming another dimensionless blowing parameter V_0/u_*. In addition, the velocity profiles normalized by the friction velocity failed to collapse. The friction velocity u_* has been used by Clauser[4] and others to normalize the outer deficit profiles in studies of both nontranspired and transpired turbulent boundary-layer flows.

In the classical theory, it was proposed that a single velocity scaling exists in the overlap region of the turbulent boundary layer with and without an external pressure gradient. Moreover, it was expected that this single velocity scaling would collapse the profiles into a single curve, thus demonstrating that both the outer and inner regions are independent of the Reynolds number. For boundary layers subjected to pressure gradients, Clauser defined an equilibrium flow as one where the pressure gradient parameter β is given by

$$\beta = \frac{\delta_*}{\rho u_*^2}\frac{\mathrm{d}P_\infty}{\mathrm{d}x} = \text{constant} \tag{3}$$

Received 22 March 2003; revision received 27 January 2005; accepted for publication 7 February 2005.

*Graduate Student, Department of Mechanical, Aerospace and Nuclear Engineering.
†Associate Professor, Department of Mechanical, Aerospace and Nuclear Engineering. Member AIAA.

and where the outer mean deficit profiles normalized by the friction velocity must be independent of the Reynolds number. This specific set of conditions led Clauser to conclude that few flows are indeed in equilibrium and that most adverse-pressure-gradient (APG) flows are nonequilibrium.

More recently, Thomas and Hasani[5] showed that the mean velocity deficit profiles normalized as

$$\left(u^{++} - U_{\infty}^{++}\right) = f_0(\bar{y}) \tag{4}$$

where

$$u^{++} = U/U^{**}, \qquad U_{\infty}^{++} = U_{\infty}\big/U^{**}$$

and

$$U^{**} = u_*(1 + \beta + B_2)^{\frac{1}{2}}$$

where the blowing parameter B_2, shown in Eq. (2) was previously defined by Andersen et al.[2] This scaling improves the collapse of the profiles subjected to an external pressure gradient and transpiration. The Clauser parameter β was included in the scaling and defined in Eq. (3). Notice that U^{**} depends on both the pressure parameter and the blowing parameter. For zero-pressure-gradient (ZPG) flows without transpiration, this scaling yields the classical scaling. More importantly, this empirical scaling will be used in this paper for comparison with the classical scaling, the Castillo/George[6] scaling (CG) and the Zagarola/Smits[7] scaling (ZS). Moreover, the scaling proposed by Thomas/Hasani[5] (TH) fails to collapse the data when the parameters $\beta + B_M \geq -1$ and the scaling $U^{**} \to \infty$ when $\beta + B_M = -1$.

Sucec and Oljaca[8,9] used integral methods to solve for the velocity profile and the skin-friction coefficient, but failed to present any plots of the velocity profiles for this problem of transpiration. Kim and Sung[10] looked at the effects of blowing or suction using direct numerical simulation. Their results follow the trends of a study done by Antonia et al.,[11] where the effect of suction on a low-Reynolds-number turbulent boundary layer was examined. Although the Reynolds stresses and wall shear stress were measured, the profiles failed to collapse into a single curve when normalizing using the friction velocity and the kinematic viscosity.

Therefore, the goal of this investigation is to use similarity analysis of the equations of motion to determine the scaling for the outer flow and to find the asymptotic velocity profile for turbulent boundary layers subjected to suction or blowing. It is also of interest to investigate the influence of suction, blowing, pressure gradient, and upstream conditions on the outer flow. Furthermore, it will be shown that the mean deficit velocity profiles normalized by the freestream velocity U_{∞} collapse the data, but to different curves for ZPG and APG. This is true as long as the upstream conditions are kept fixed (i.e., upstream wind-tunnel speed). Additionally, it will be demonstrated that the value of the pressure parameter Λ for the boundary layer subject to APG in a transpired flow is not the same as the value found in Castillo and George,[6] that is, $\Lambda \equiv [\delta/\rho U_{\infty}^2(\mathrm{d}\delta/\mathrm{d}x)](\mathrm{d}P_{\infty}/\mathrm{d}x) \cong 0.22$, and it is directly affected by the strength of the blowing parameter V_0^+. It will also be confirmed that the blowing parameter directly affects the behavior of the downstream flow.

II. Similarity Analysis

The scales for different quantities in the turbulent boundary layer are obtained when the equilibrium similarity analysis is applied to the governing equations. George and Castillo[12] applied this concept to the Reynolds-averaged Navier–Stokes (RANS) equations in order to determine the mean velocity and Reynolds stresses scales in the outer flow of a ZPG turbulent boundary layer. A similar approach is adopted here for the outer turbulent boundary layer subjected to transpiration and an external pressure gradient.

A. Outer-Boundary-Layer Equations

The equations of motion and boundary conditions for the outer part ($\bar{y} > 0.1$ or $y^+ = 0.1\delta^+$ where $\delta^+ = \delta u_*/\nu$) of a pressure gradient turbulent boundary layer (with constant properties) at high Reynolds number are given as

$$\frac{\partial U}{\partial x} + \frac{\partial V}{\partial y} = 0 \tag{5}$$

$$U\frac{\partial U}{\partial x} + V\frac{\partial U}{\partial y} = -\frac{1}{\rho}\frac{\mathrm{d}P_{\infty}}{\mathrm{d}x} + \frac{\partial}{\partial y}[-\langle uv\rangle] \tag{6}$$

where $U = 0, V = V_0$ as $y = 0$ and $U \to U_{\infty}, -\langle uv\rangle \to 0$ as $y \to \infty$. This complete set of equations, boundary conditions, and its development into the outer equation have been described in detail by Tennekes and Lumley[13] for a ZPG turbulent boundary layer and by Castillo and George[6] for a pressure-gradient turbulent boundary layer. Notice that the gradients of the viscous terms and normal stresses in the momentum equation have been neglected because they are second-order terms compared to the inertial and Reynolds shear-stress terms. This is true for APG flows far from separation.[14] For a finite Reynolds number, the gradient of the viscous terms plays a role in the region near the wall of the boundary layer as shown by Wei et al.[15] This inner region is composed of the viscous sublayer, the buffer layer, and the overlap region. More important, the region where the viscous terms are important outside of the viscous sublayer region has been precisely defined by George and Castillo[12] as the mesolayer region ($30 \leq y^+ \leq 300$).

For boundary layers with transpiration, the integral boundary-layer equation is given as

$$\frac{C_f}{2} = \frac{\mathrm{d}\theta}{\mathrm{d}x} + \frac{\theta}{U_{\infty}}\frac{\mathrm{d}U_{\infty}}{\mathrm{d}x}(2 + H) - \frac{V_0}{U_{\infty}} \tag{7}$$

where the friction factor C_f can be directly computed from this equation, which takes into account the effect of the vertical velocity at the wall V_0.

B. Similarity Solution Form

It is assumed that the velocity and Reynolds shear stress can be written in terms of a product solution of two functions. The outer mean velocity deficit $U_{\infty} - U$ and the Reynolds shear stress are expressed as

$$U_{\infty} - U = U_{\mathrm{so}}(x) f_{\mathrm{op}}\left(\bar{y}, \delta^+, \Lambda, V_0^+, *\right) \tag{8}$$

$$-\langle uv\rangle = R_{\mathrm{so}_{uv}}(x) r_{\mathrm{op}_{uv}}\left(\bar{y}, \delta^+, \Lambda, V_0^+, *\right) \tag{9}$$

where U_{so} and $R_{\mathrm{so}_{uv}}$ depend on x only and need to be determined from the equations of motion and boundary conditions. The arguments inside the similarity functions f_{op} and $r_{\mathrm{op}_{uv}}$ represent the outer similarity coordinate $\bar{y} = y/\delta_{95}$, the Reynolds-number dependence $\delta^+ = \delta u_*/\nu$, the pressure gradient parameter Λ, the blowing parameter V_0^+, and any possible dependence on the upstream conditions $*$, respectively. Some of the upstream conditions can include the upstream wind-tunnel speed U_0, the turbulence intensity, or the geometry and size of the tripping device to mention a few. The pressure parameter and the blowing parameter are both determined in a subsequent section as a consequence of the similarity constraints. The blowing parameter is studied in the remaining parts of this paper in order to understand the effects of this parameter on the downstream flow.

C. Asymptotic Invariance Principle

This principle is based on the fact that in the limit as the Reynolds number approaches infinity the turbulent boundary-layer equations become Reynolds-number invariant. Because in the infinite Reynolds-number limit, the outer equations become independent of δ^+, and so must the properly scaled solutions to them. Hence, in this

limit Eqs. (8) and (9) must also become independent of Reynolds number; thus,

$$f_{\mathrm{op}}\left(\bar{y}, \delta^+, \Lambda, V_0^+, *\right) \rightarrow f_{\mathrm{op}\infty}\left(\bar{y}, \Lambda, V_0^+, *\right) \tag{10}$$

$$r_{\mathrm{op}_{uv}}\left(\bar{y}, \delta^+, \Lambda, V_0^+, *\right) \rightarrow r_{\mathrm{op}\infty_{uv}}\left(\bar{y}, \Lambda, V_0^+, *\right) \tag{11}$$

The subscript op∞ is used to establish the difference between these infinite Reynolds-number solutions and the finite Reynolds-number solutions in Eqs. (8) and (9). In the following sections, it will be shown that when ZPG and APG boundary layers are normalized by the Zagarola/Smits scaling $U_\infty(\delta_*/\delta)$, the effects of blowing parameter, upstream conditions, and the strength of the pressure gradient are nearly removed from the outer flow. This result is very important because the true asymptotic profiles for ZPG and APG can be found even at finite Reynolds number.

D. Transformed Similarity Equation

Using the asymptotic functions shown in Eqs. (10) and (11), it is feasible to obtain an outer scaling along with various constraints for the outer flow. Substituting these equations into Eq. (6), the partial differential equation is converted into a second-order differential equation and is given as

$$\begin{aligned}
&\left[\delta\frac{\mathrm{d}U_\infty}{\mathrm{d}x}+\frac{\delta U_\infty}{U_{\mathrm{so}}}\frac{\mathrm{d}U_{\mathrm{so}}}{\mathrm{d}x}\right]f_{\mathrm{op}\infty}+\left[\delta\frac{\mathrm{d}U_{\mathrm{so}}}{\mathrm{d}x}\right]f_{\mathrm{op}\infty}^2\\
&\quad+\left[U_\infty\frac{\mathrm{d}\delta}{\mathrm{d}x}+\delta\frac{\mathrm{d}U_\infty}{\mathrm{d}x}\right]\bar{y}f'_{\mathrm{op}\infty}+\left[U_{\mathrm{so}}\frac{\mathrm{d}\delta}{\mathrm{d}x}-\delta\frac{\mathrm{d}U_{\mathrm{so}}}{\mathrm{d}x}\right]f'_{\mathrm{op}\infty}\\
&\quad\times\int_{\bar{y}}^{1}f_{\mathrm{op}\infty}(\tilde{y})\,\mathrm{d}\tilde{y}+\left[V_0-\delta\frac{\mathrm{d}U_\infty}{\mathrm{d}x}\right]f'_{\mathrm{op}\infty}+\left[\frac{\delta U_\infty}{U_{\mathrm{so}}}\frac{\mathrm{d}U_\infty}{\mathrm{d}x}\right]\\
&\quad=-\left[\frac{1}{\rho}\frac{\mathrm{d}P_\infty}{\mathrm{d}x}\right]-\left[\frac{R_{\mathrm{so}_{uv}}}{U_{\mathrm{so}}}\right]r'_{\mathrm{op}\infty_{uv}}
\end{aligned}\tag{12}$$

To have an equilibrium boundary layer as defined by Castillo and George,[6] all of the terms in square brackets must maintain a relative balance between each other as the flow develops. Therefore, equilibrium similarity solutions exist only if all of the terms within the square brackets possess the same x dependence and are also independent of the similarity coordinate $\bar{y}$. Consequently,

$$\begin{aligned}
&\underbrace{\delta\frac{\mathrm{d}U_\infty}{\mathrm{d}x}}_{1}\sim\underbrace{\frac{\delta U_\infty}{U_{\mathrm{so}}}\frac{\mathrm{d}U_{\mathrm{so}}}{\mathrm{d}x}}_{2}\sim\underbrace{\delta\frac{\mathrm{d}U_{\mathrm{so}}}{\mathrm{d}x}}_{3}\sim\underbrace{U_\infty\frac{\mathrm{d}\delta}{\mathrm{d}x}}_{4}\sim\underbrace{U_{\mathrm{so}}\frac{\mathrm{d}\delta}{\mathrm{d}x}}_{5}\\
&\quad\sim\underbrace{V_0}_{6}\sim\underbrace{\frac{1}{\rho}\frac{\mathrm{d}P_\infty}{\mathrm{d}x}}_{7}\sim\underbrace{\frac{R_{\mathrm{so}_{uv}}}{U_{\mathrm{so}}}}_{8}
\end{aligned}\tag{13}$$

The symbol $\sim$ denotes that the terms are proportional to each other; thus, a relative balance should remain among them as the flow evolves. The scales for the outer flow are determined in this limit as $Re\rightarrow\infty$. Using terms 4 and 5 from Eq. (13), the outer velocity U_{so} yields into

$$U_{\mathrm{so}}\sim U_\infty \tag{14}$$

and from terms 4 and 8 along with Eq. (14), it follows that

$$R_{\mathrm{so}_{uv}}\sim U_\infty^2\frac{\mathrm{d}\delta}{\mathrm{d}x} \tag{15}$$

These scalings for the mean deficit profiles and Reynolds shear stress are the same for a transpired flow and a nontranspired flow. However, there are some new constraints, which arise as a result of the imposed blowing velocity.

E. Additional Constraints

A set of constraints pertaining to the problem of turbulent boundary layers subjected to transpiration has been found after applying the equilibrium similarity analysis to the equations of motion. For example, the blowing parameter is defined from the terms 4 and 6 in Eq. (13) as

$$V_0^+=\frac{V_0}{U_\infty(\mathrm{d}\delta/\mathrm{d}x)} \tag{16}$$

Similarly, the pressure parameter Λ must be a constant obtained from terms 1 and 4 or from terms 4 and 7 in Eq. (13). Consequently, the constraint for the pressure parameter is given as

$$\Lambda\equiv-\frac{\delta}{U_\infty(\mathrm{d}\delta/\mathrm{d}x)}\frac{\mathrm{d}U_\infty}{\mathrm{d}x}\equiv\frac{\delta}{\rho U_\infty^2(\mathrm{d}\delta/\mathrm{d}x)}\frac{\mathrm{d}P_\infty}{\mathrm{d}x}=\text{constant} \tag{17}$$

which is a necessary condition for an equilibrium flow to exist.[6] When this Eq. (17) is integrated for nonzero values of Λ, a power relation between δ and U_∞ succumbs into

$$\delta\sim U_\infty^{-1/\Lambda} \tag{18}$$

for equilibrium flows. Consequently, if the data expressed in $\log(U_\infty)$ vs $\log(\delta)$ are plotted, a linear relationship between these two quantities must exist if the flow is in equilibrium, thus yielding the pressure parameter Λ as the slope. Surprisingly, Castillo and George[6] and Castillo et al.[16] were able to show that many pressure-gradient boundary layers are indeed equilibrium boundary layers and that the exceptions are nonequilibrium turbulent boundary layers. The mentioned theory remains standing and applies even for flows that are close to separation. More specifically, they showed that the value of Λ for turbulent boundary layers subject to APG is $\Lambda\cong 0.22$. In a transpired turbulent boundary-layer flow subjected to pressure gradient, the value of Λ is directly influenced by the blowing velocity and can also be described as

$$\Lambda_\beta\equiv\frac{\delta}{\rho U_\infty V_0}\frac{\mathrm{d}P_\infty}{\mathrm{d}x}=\text{constant} \tag{19}$$

This transpired pressure parameter can be written in terms of the pressure parameter Λ as

$$\Lambda_\beta\equiv\Lambda\Big/V_0^+=\text{constant} \tag{20}$$

Because $\Lambda=$ constant for equilibrium flows, the blowing pressure parameter Λ_β is directly influenced by the blowing velocity imposed at the wall.

III. Zagarola/Smits Scaling

After George and Castillo[12] and Castillo and George[6] applied the similarity analysis to the boundary layer on ZPG and APG flows, respectively, they showed that the overlap layer is characterized by two velocity scalings and not a single scale as in the classical theory. Consequently, the overlap layer is Reynolds-number dependent, and in the case of suction or blowing the dependence on the blowing parameter V_0^+ must be included.

ZS[7] provided an empirical scaling that could collapse the mean deficit velocity profiles into a single curve given by $U_\infty(\delta_*/\delta)$. The derivation and proof of this scaling was performed by Castillo.[17] Furthermore, this scaling has been applied to several problems such as boundary layer with roughness[18] as well as turbulent boundary layers subject to changes in the upstream conditions.[19] Consequently, the objective of this section is to find the true asymptotic profiles for ZPG and PG flows subject to transpiration at finite Reynolds number. It will be assumed that the same function from the similarity analysis f_{op} can now be expressed as a product of two functions:

$$f_{\mathrm{op}}\left(\bar{y}, \delta^+, \Lambda, V_0^+, *\right)=G\left(\delta^+, V_0^+, *\right)f_{\mathrm{op}\infty}(\bar{y}, \Lambda) \tag{21}$$

The function G possesses the dependence on the local Reynolds number δ^+, the blowing parameter V_0^+, and the upstream conditions $*$. The inclusion of the blowing parameter in the first function

of f_{op} is the main difference in the derivation. On the other hand, the asymptotic similarity function $f_{\text{op}\infty}$ includes the similarity length scale $\bar{y}$ and the pressure parameter Λ. Therefore, this function $f_{\text{op}\infty}$ represents the true asymptotic velocity profile, which should be independent of Reynolds number, but the shape of the profile can change depending on type of pressure gradient (ZPG, APG or favorable pressure gradient). This shape is closely related and dependent on the value of the pressure parameter Λ. A similar approach of decomposing the profile was done by Castillo[17] and Wosnik and George.[20]

Using the displacement thickness defined as

$$U_\infty \delta_* = \int_0^\infty (U_\infty - U)\,\mathrm{d}y \tag{22}$$

for an incompressible flow and the similarity function in Eq. (21), the function G is obtained. In the limit as the Reynolds number goes to infinity, it follows that

$$[\delta_*] \approx [\delta G] \int_0^1 f_{\text{op}\infty}(\bar{y}, \Lambda)\,\mathrm{d}\bar{y} \tag{23}$$

As mentioned earlier, the inner part of the boundary layer is not taken into account in the analysis, but there is a small contribution at finite Reynolds number. The terms in square brackets must be proportional to each other; thus,

$$G \propto (\delta_*/\delta) \tag{24}$$

Therefore by combining the function G with Eq. (21), the outer scaling is given as $U_{\text{so}} = U_\infty(\delta_*/\delta)$. The term that contains the Reynolds number, upstream conditions as well as the blowing parameter dependencies, is given by the ratio of the displacement thickness and the boundary-layer thickness δ_*/δ.

The asymptotic invariance principle (AIP) demands that any similarity function that is properly scaled should be asymptotically independent of the Reynolds number; thus, in the limit as $\delta^+ \to \infty$, the function $G \to G_\infty$ is equal to a constant. If this proposed decomposition of f_{op} is valid, then all of the effects of upstream conditions, strength of pressure gradient, and transpiration should be removed by the ZS scaling.

IV. Experimental Data

The experimental data acquired by Andersen et al.[2] using hot-wire anemometry are used to compare the classical scaling, the scaling proposed by TH[5] the CG[6] scaling, and the ZS[7] scaling. Table 1 shows a summary of the classical scaling (first row), the TH scaling

Table 1 Outer scalings

Investigator	Scaling: U_{so}	Length scale
Classical scaling $(U_\infty - U)/U_{\text{so}}$	$U_{\text{so}} = u_*$	y/δ_{95}
Thomas/Hasani $(U_\infty - U)/U_{\text{so}}$	$U_{\text{so}} = (u^{++} - U_\infty^{++})$	y/δ_{95}
Castillo/George $(U_\infty - U)/U_{\text{so}}$	$U_{\text{so}} = U_\infty$	y/δ_{95}
Zaragola/Smits $(U_\infty - U)/U_{\text{so}}$	$U_{\text{so}} = U_\infty(\delta_*/\delta)$	y/δ_{95}

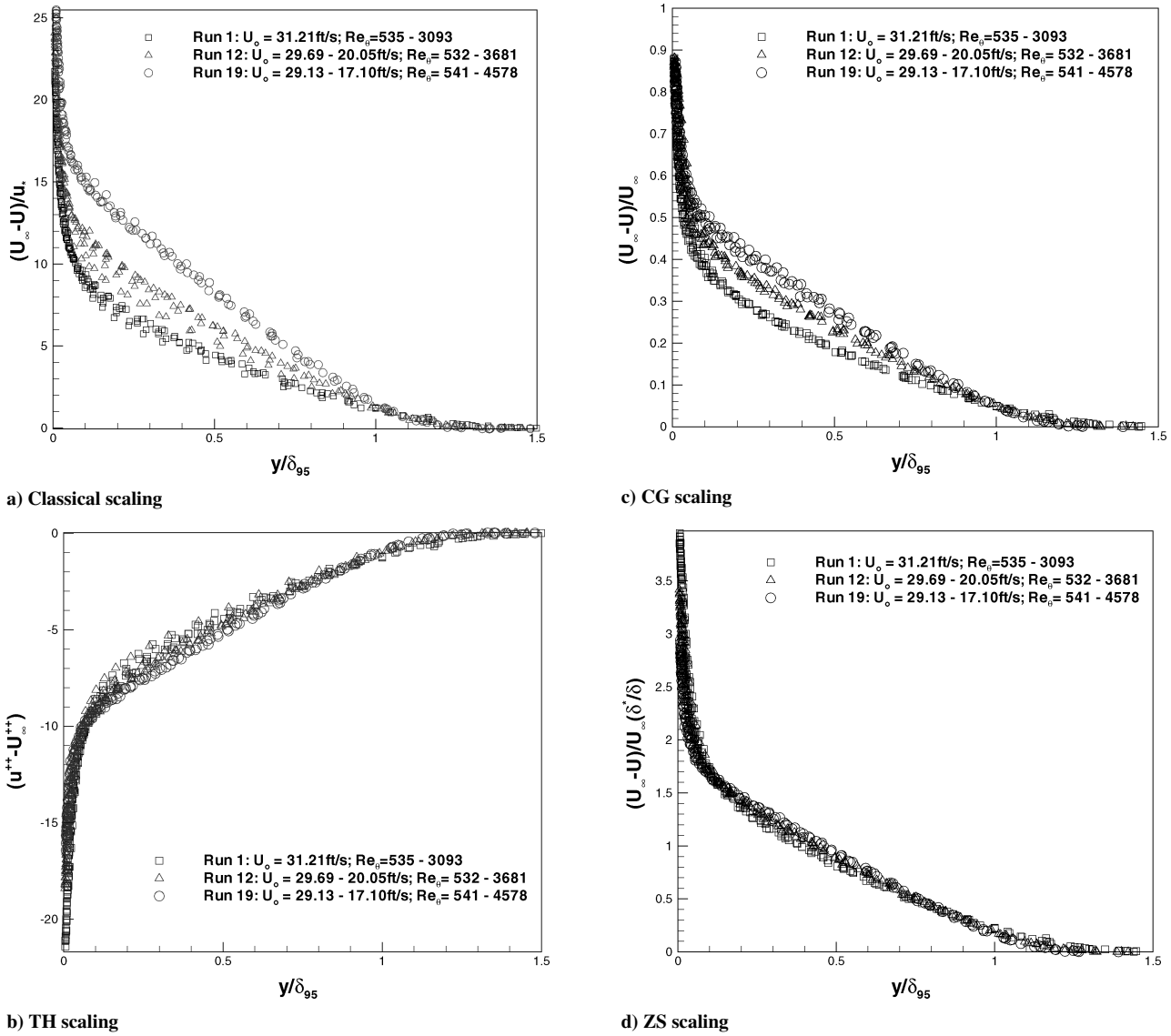

a) Classical scaling

c) CG scaling

b) TH scaling

d) ZS scaling

Fig. 1 Mean velocity deficit profiles in ZPG and APG without transpiration.

shown in the following row, the CG scaling in the third row, and the ZS scaling in the last row. The TH scaling is a modification of the classical scaling, whereas the ZS scaling is an actual extension of the GC scaling.

The ZPG experimental data have a freestream velocity of 31 ft/s. The APG data are obtained for freestream velocities of 29 ft/s and are reduced to 17 ft/s. There is a power relationship between the freestream velocity and the streamwise distance of the form $U_\infty \sim x^m$. For the APG experimental data, the values of the power are given as $m = -0.15$ and -0.20, thus forming a mild and a strong APG flow. Furthermore, the power m represents the strength of the pressure gradient. Moreover, the magnitudes of the blowing parameter $V_0^+ = V_0/U_\infty(\mathrm{d}\delta/\mathrm{d}x)$, as defined by the similarity analysis, vary from -0.440 to 0.589. Blowing is represented by $V_0^+ > 0$, whereas suction is represented by $V_0^+ < 0$. The Reynolds number based on momentum thickness Re_θ ranges from 567 up to 10.8×10^3. Each run or set of measurements has different conditions of transpiration or pressure gradient cases as tabulated in Table 2.

Table 2 Data cases and conditions for different runs

Effect	ZPG	Mild APG	Strong APG
Suction	Not considered	Runs 7–11	Run 20
Blowing	Runs 2–5	Runs 13–18	Not considered
Nontranspired	Run 1	Run 12	Run 19

V. Results

A. Velocity Profiles Without Transpiration

Figure 1 shows the mean deficit velocity profiles for nontranspired flows subjected to ZPG and APG including two different strengths of adverse pressure gradient. Data runs 1, 12, and 19 are taken from Andersen et al.[2] These particular cases vary in Reynolds number based on momentum thickness from about $850 \leq Re_\theta \leq 3.7 \times 10^3$.

Figure 1a shows the profiles normalized using the classical scaling u_* and δ_{95}. Notice that in the classical view the profiles should collapse into a single curve. This figure clearly shows the opposite effect. However, Fig. 1b shows the same experimental data normalized by the TH scaling. Notice that this scaling contains the effects of the pressure gradient given by the Clauser parameter β and the blowing parameter B_2. Even though the profiles collapse better than with the classical scaling, there is some residual dependence on the Reynolds number. In Fig. 1c, the profiles are normalized by the CG scaling. Notice that the profiles collapse, but to different curves showing the effect caused by the external pressure gradient. In fact, these are called self-similar solutions because the profiles collapse for a given set of upstream conditions, but the shape changes for each of the three runs shown. Finally when the ZS scaling shown in Fig. 1d is used, the profiles collapse to one single curve. More importantly, this scaling nearly removes all effects. The small residual difference in the profiles is caused by the strength of the pressure gradient. Castillo and Walker[19] showed that the asymptotic profiles

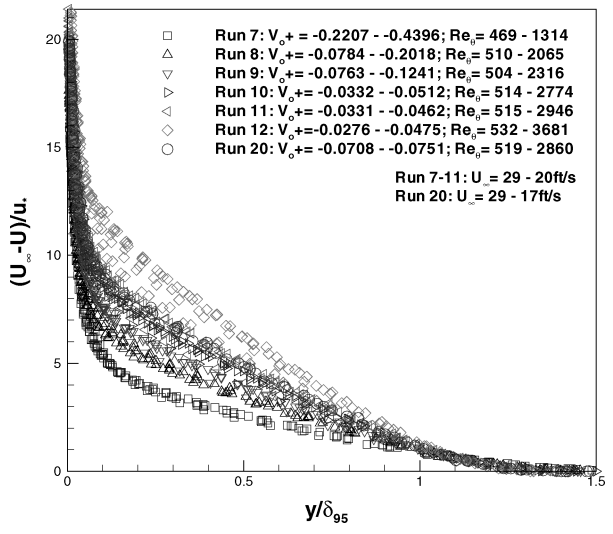

a) Classical scaling

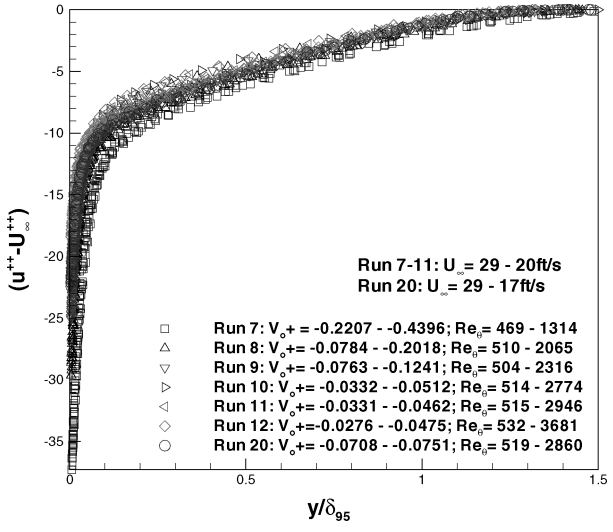

b) TH scaling

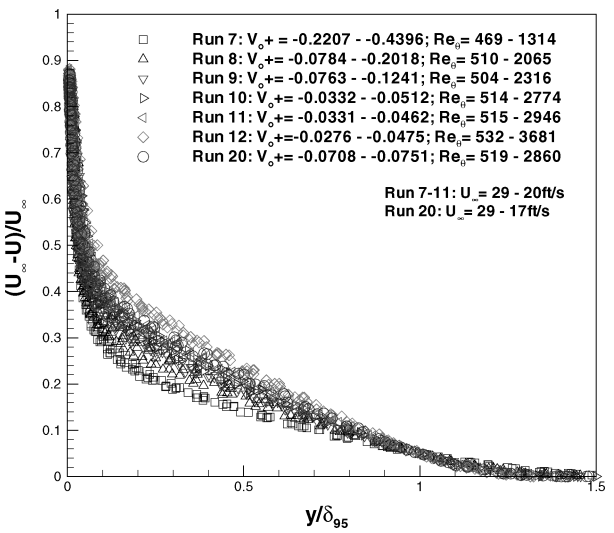

c) CG scaling

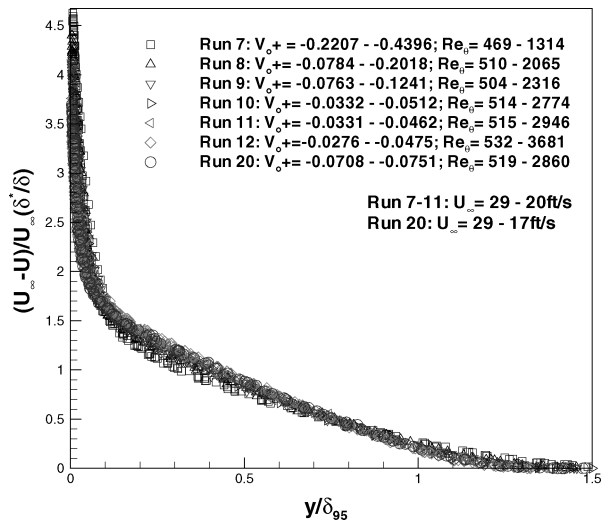

d) ZS scaling

Fig. 2 Mean velocity deficit profiles in APG with suction.

found using the ZS scaling for APG and ZPG are different; thus, the present results are consistent with their findings. The boundary-layer thickness at $U/U_\infty = 0.95$ has been used as the length scale δ_{95} for all profiles shown in this paper.

B. Velocity Profiles with Suction

Figure 2 shows the mean deficit velocity profiles subject to suction in APG flows. The data used for these profiles, runs 7–11 and run 20, are taken from Andersen et al.[2] The blowing parameter V_0^+ ranges from -0.028 to -0.440, and the Reynolds number based on momentum thickness varies from 469 up to 3.7×10^3.

Figure 2a shows the APG profiles with suction using the classical scaling u_*. This friction velocity was obtained from the slope at the wall and confirmed by the friction factor value from the experimental data. Notice that the classical scaling fails to collapse the profiles. However, the velocity profiles shown in Fig. 2b normalized with the TH scaling show a better collapse than both the classical scaling and the CG scaling shown in Fig. 2c. Furthermore, notice that when the CG scaling is used the profiles collapse to different curves, thus obtaining self-similar solutions for each experiment. The effects seen in Fig. 2c are caused by the strength of the blowing parameter and the strength of the pressure gradient. The more negative the parameter (increase in suction), the closer the profiles move toward to the wall. Notice that run 20 is clearly distinguishable from the others, and it remains positioned above the other measurements because it has a stronger adverse pressure gradient. More importantly, notice the excellent collapse of the profiles using the ZS scaling as shown in Fig. 2d. Clearly, the effects of the blowing parameter and pressure gradient are nearly removed from the outer flow. Therefore, this profile represents the asymptotic profile for APG flows with suction at finite Reynolds number.

C. Velocity Profiles with Blowing

Figure 3 shows the mean deficit velocity profiles subject to blowing in ZPG and APG flows. Data runs 2–5 and runs 13–18 from Andersen et al.[2] correspond to ZPG and APG, respectively. The blowing parameter value ranges from 0.025 to 0.589, and the Reynolds number based on momentum thickness ranges from about $500 \le Re_\theta \le 10.8 \times 10^3$.

Figure 3a shows the mean deficit velocity profiles normalized using the classical scaling. Notice that the profiles do not collapse as expected from the classical theory, consequently showing dependencies on the Reynolds number and blowing parameter V_0^+. The same experimental data normalized by the TH scaling are shown in Fig. 3b. Although the profiles tend to collapse and improve significantly when compared with the classical scaling, there is still some variation in the outer region caused by the pressure gradient, blowing parameter, and Reynolds number. Figure 3c shows the mean deficit velocity profiles scaled with the CG scaling based on the freestream velocity. Notice that as the blowing parameter increases, the profiles tend to move away from the wall. More interestingly, the profiles

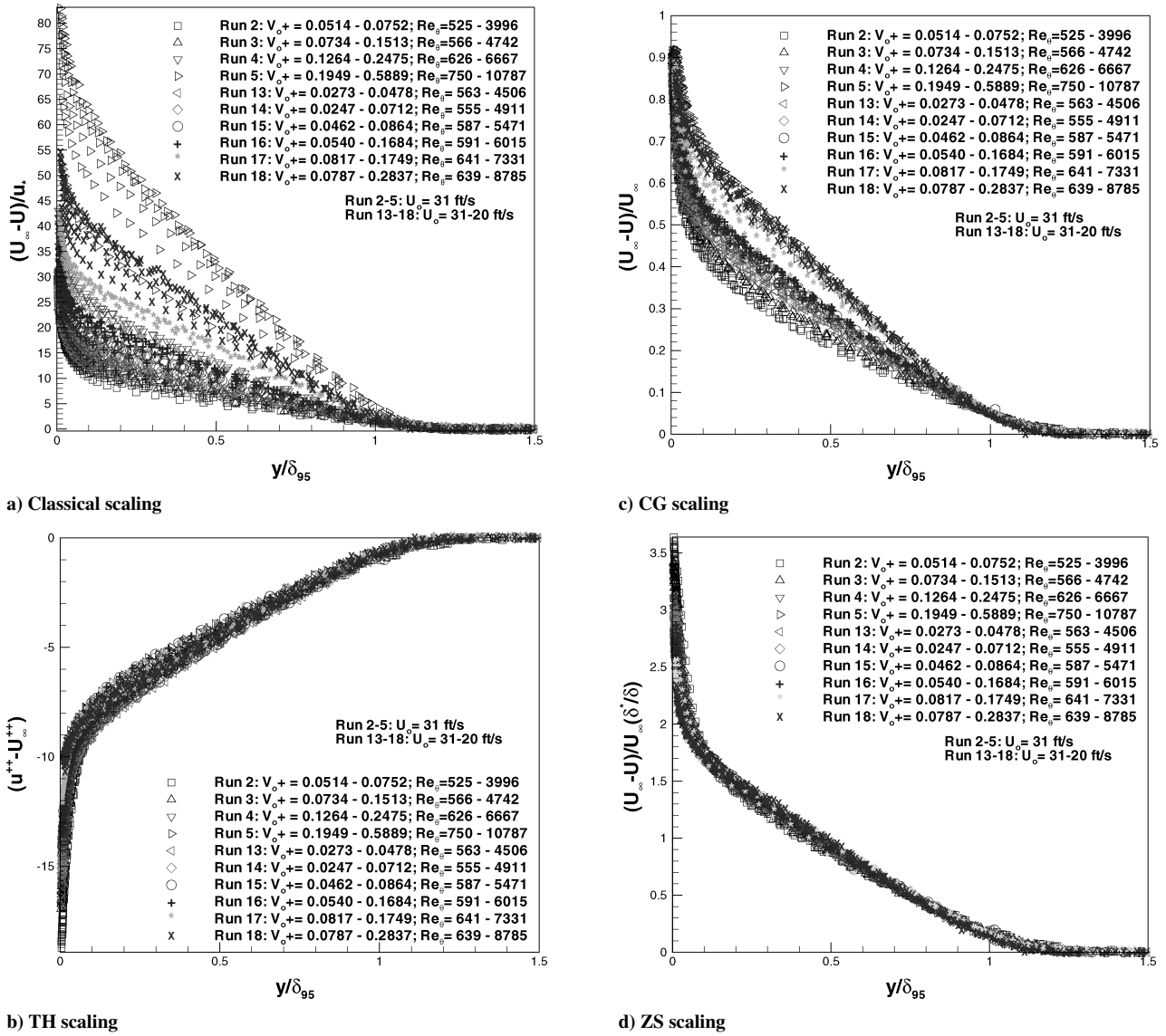

a) Classical scaling

c) CG scaling

b) TH scaling

d) ZS scaling

Fig. 3 Mean velocity deficit profiles in ZPG and APG with blowing.

collapse for a given set of conditions (i.e., blowing parameter and upstream wind-tunnel speed), but to different curves. This indeed demonstrates again the influence of the blowing parameter on the profiles in the outer flow. In the bottom of Fig. 3d, the profiles are now normalized using the ZS scaling $U_\infty(\delta_*/\delta)$. Clearly, the ratio of displacement thickness and boundary-layer thickness δ_*/δ nearly removes the effects of the blowing parameter, external pressure gradient, upstream conditions, and Reynolds number from the outer flow; thus, the asymptotic profile is found even at finite Reynolds number.

D. ZPG Velocity Profiles

Figure 4 shows the mean deficit velocity profiles for ZPG with and without blowing. The range for the Reynolds number based on the momentum thickness varies from $500 \leq Re_\theta \leq 10.8 \times 10^3$, and the blowing parameter V_0^+ ranges from $0 \leq V_0^+ \leq 0.589$.

In Fig. 4a, the mean deficit velocity profiles are normalized with the classical scaling. The observed profiles fail to collapse, even though there is no effect from the external pressure gradient. Meanwhile, the collapse of the profiles using the TH scaling shown in Fig. 4b improves drastically when modifying the scaling from the classical scaling to the TH scaling. The profiles using the CG scaling shown in Fig. 4c do not collapse as well as the TH scaling. However, observe that for a given blowing range the shape of the profiles is affected, but there is still a collapse into different curves depending on each given set of conditions. (i.e., upstream wind-tunnel speed, blowing parameter, etc.) As mentioned earlier, these are recognized as self-similar solutions, whereas the profiles normalized by the ZS scaling yield the self-preserving solutions sought by Townsend.[21]

As the blowing parameter increases, the profiles move away from the wall and are independent of Reynolds number. Furthermore, when the same experimental data are normalized by the ZS scaling as shown in Fig. 4d, the profiles nearly collapse onto a single curve. This scaling removes almost all of the effects on the outer flow caused by the blowing parameter. However, notice that the shape of the asymptotic profile is slightly different for the profiles with blowing than those without the blowing effect. This observation leads to the conclusion that the asymptotic profiles for nontranspired and blowing are quite different as it is the case of ZPG and APG flows. Using the similarity analysis and the ZS scaling, Castillo and Walker showed that there are three profiles in boundary layers: one for ZPG flows, one for FPG flows, and one for APG flows.

E. APG Velocity Profiles

Figure 5 shows the mean deficit velocity profiles for APG subject to suction and blowing. The blowing parameter varies from -0.440 to 0.284, representing a wide spectrum in conditions from suction to blowing. The Reynolds number based on momentum thickness ranges from about $450 \leq Re_\theta \leq 9 \times 10^3$.

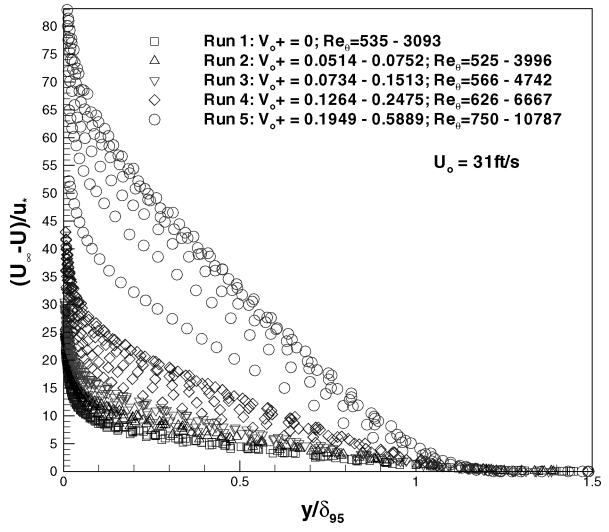

a) Classical scaling

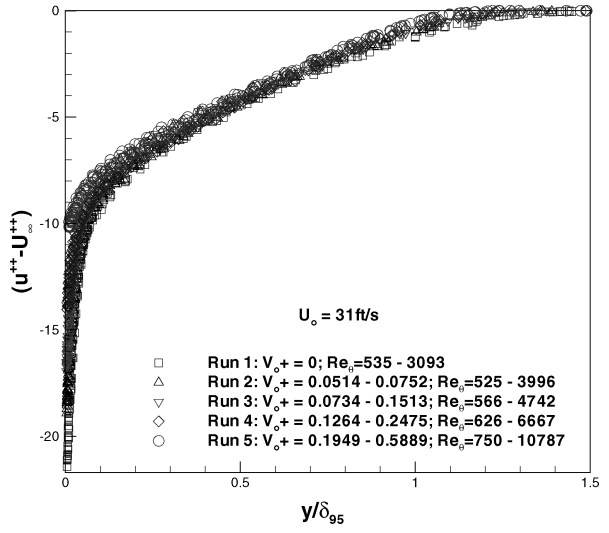

b) TH scaling

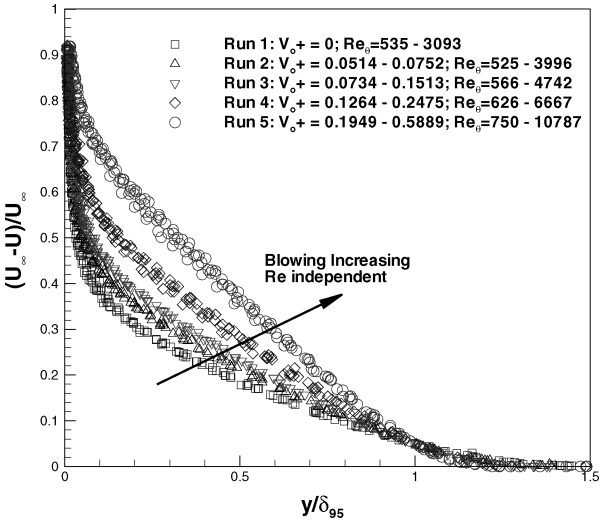

c) CG scaling

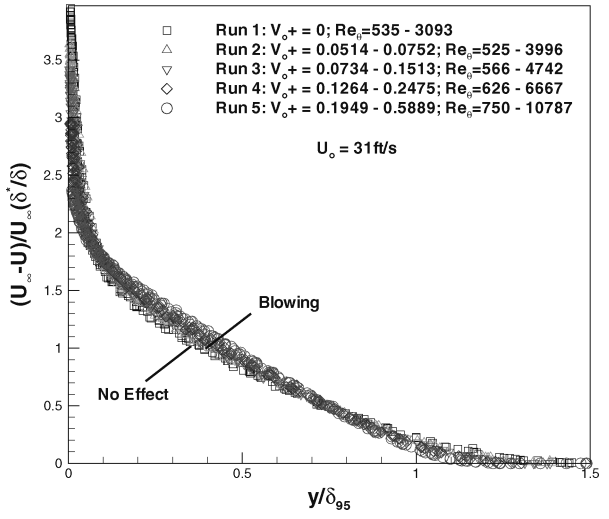

d) ZS scaling

Fig. 4 Mean velocity deficit profiles in ZPG with and without blowing.

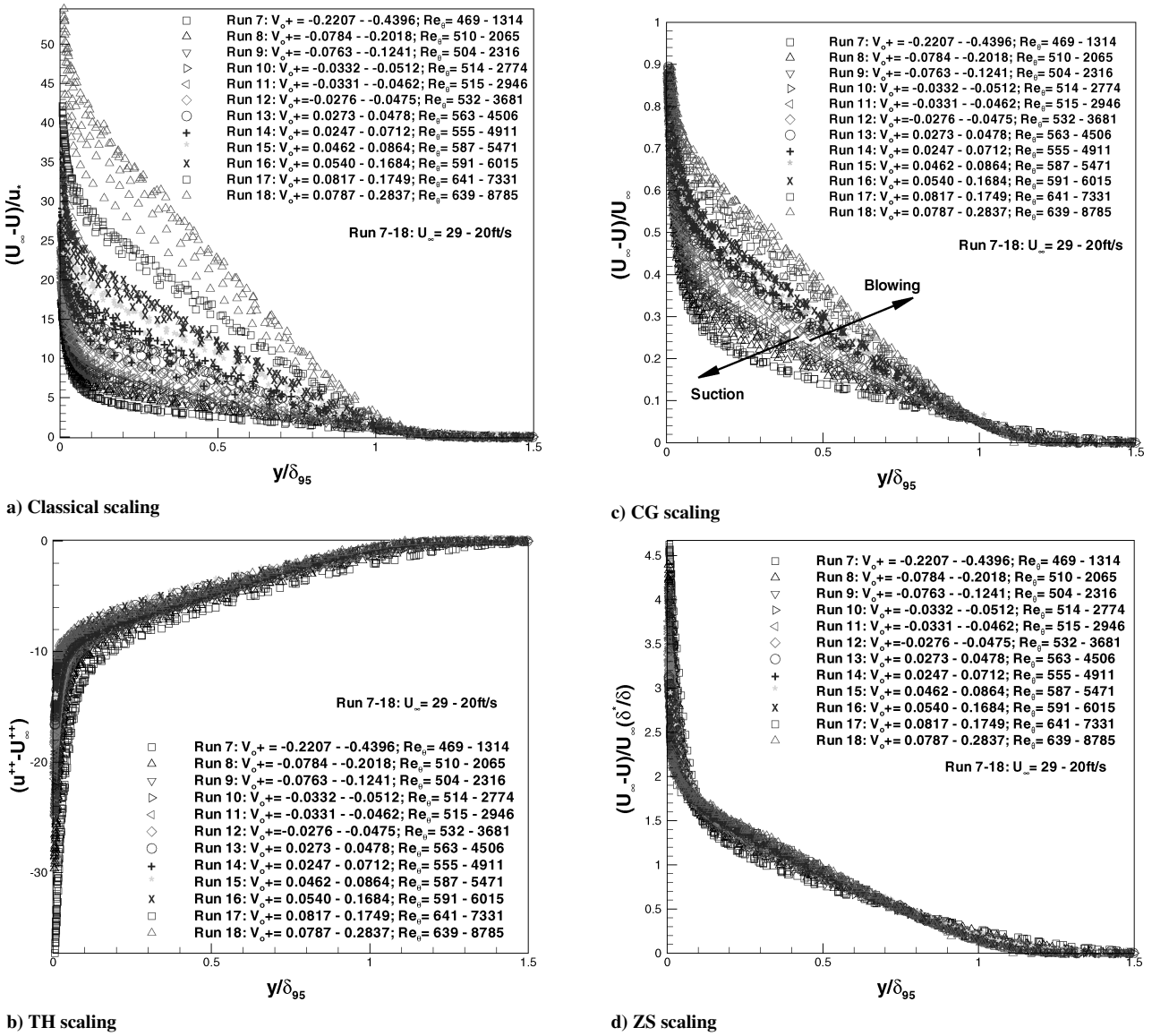

Fig. 5 Mean velocity deficit profiles in APG with and without transpiration.

Figure 5a shows the mean deficit profiles normalized by the classical scaling. As with the rest of the profiles, the data fail to collapse when normalized by the friction velocity u_*, even when the strength of the pressure gradient is small, given that only the mild APG data were used. However, the profiles using the TH scaling shown in Fig. 5b almost collapse, but not as efficiently as the ZS scaling shown in Fig. 5d. Moreover, the profiles normalized by the freestream velocity shown in Fig. 5c exhibit an interesting behavior. First, notice that the profiles collapse to a given curve depending on the strength of the blowing parameter V_0^+. Second, it is seen that as the blowing parameter increases, the profiles move away from the wall and are independent of the Reynolds number. Inversely, the opposite behavior is observed when the strength of the blowing parameter decreases as in the case of suction. On the other hand, the same data normalized by the ZS scaling of Fig. 5 show an excellent collapse. However, notice that the shape of the asymptotic profiles for suction is different from those for blowing. Therefore, the shape of these profiles is directly affected whether the flow is subjected to blowing or to suction as it was shown in the scaling by CG shown in Fig. 5c.

F. Boundary-Layer Parameters

Figure 6 shows the relation between the displacement thickness over the nominal boundary-layer thickness δ_*/δ vs the Reynolds number based on the momentum thickness Re_θ. The parameter changes over a small range of the Reynolds number in the case of the APG data shown in Fig. 6b, and it is nearly constant for the ZPG data shown in Fig. 6a.

The blowing parameter causes the δ_*/δ parameter to grow differently from run to run. Furthermore, notice that as the blowing parameter changes from suction to blowing, this boundary-layer parameter tends to increase. It is also apparent that for each individual APG run the parameter decreases locally and separately from the other cases if there is suction. Inversely, if there is blowing the parameter increases locally. More importantly, the ratio of δ_*/δ is indeed the variable included in the ZS scaling, and it captures the effects of the local Reynolds number, the strength of the pressure gradient, and the blowing parameter as well as the upstream conditions.

Figure 7 shows the growth of the boundary layer Re_δ vs Re_x. Notice that for each case, the boundary layer grows differently and increases even though the Reynolds-number range is within the same range of values. As the blowing parameter increases, the boundary layer grows faster as expected. For the data considered here, the boundary layer grows linearly. Again, it is seen in Fig. 7b that the boundary layer grows faster if the strength of the APG is increased as well as when blowing is imposed at the wall.

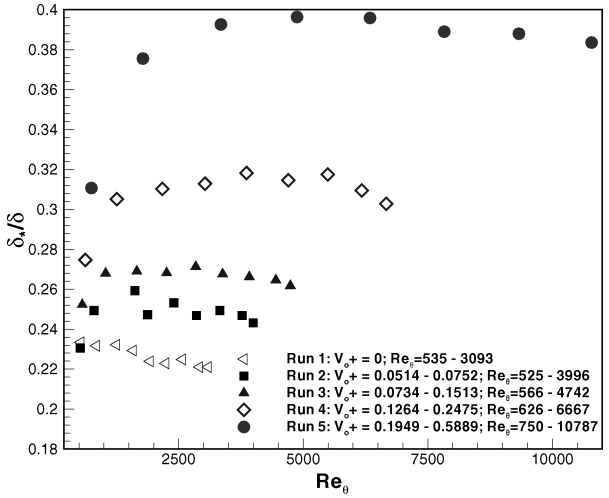

a) ZPG data with and without blowing

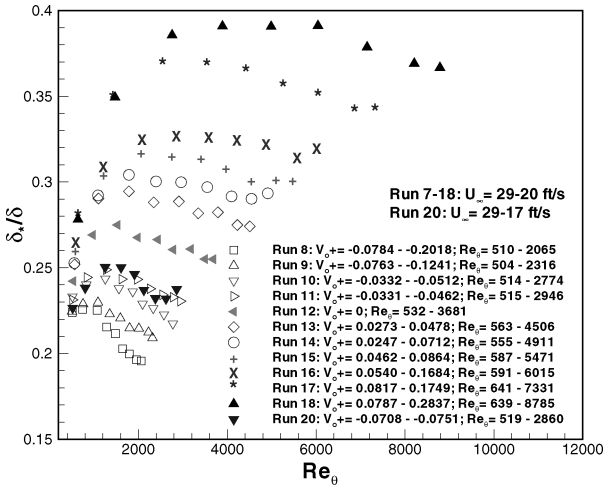

b) APG data with and without transpiration

Fig. 6 Displacement over nominal thickness δ_*/δ vs Re_θ.

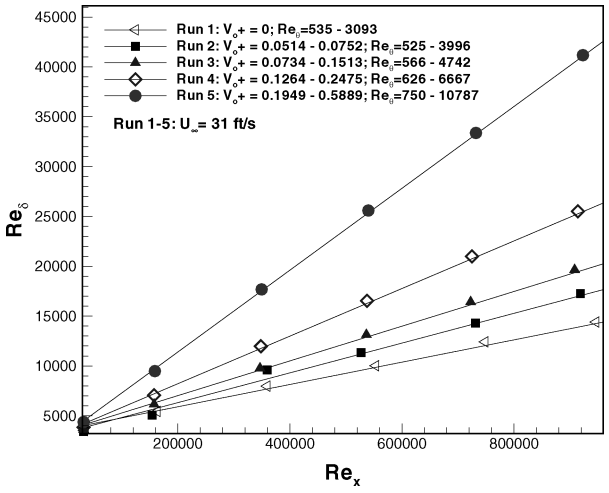

a) ZPG data with and without blowing

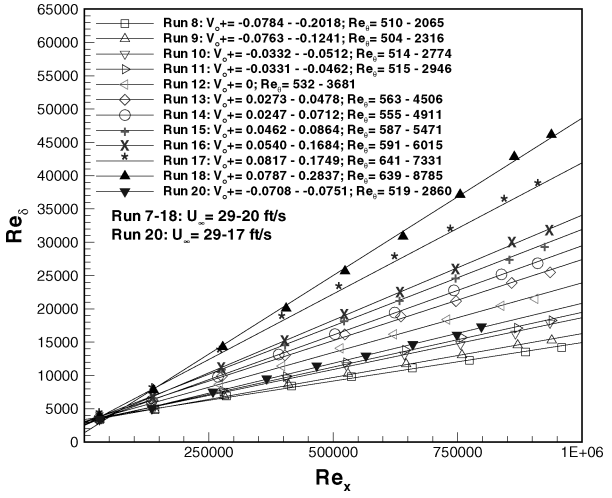

b) APG data with and without transpiration

Fig. 7 Boundary-layer growth: Re_δ vs Re_x.

G. Pressure Parameter: Λ

Using the similarity analysis of the RANS equations, Castillo et al.[16] showed that the outer part of an adverse-pressure-gradient turbulent boundary layer tends to remain in equilibrium. It was demonstrated that an equilibrium flow exists if $\Lambda =$ constant and for $\Lambda \neq 0$, $\delta \sim U_\infty^{-1/\Lambda}$. Consequently, when plotting the logarithmic quantities of U_∞ and δ, this power relation between the freestream velocity and boundary-layer thickness must be linear if an equilibrium flow exists at all. In previous investigations carried out by Castillo and George,[6] the pressure parameter was found to have a constant value of about 0.22 for equilibrium flows subjected to an APG. In the case of turbulent boundary layers with an adverse pressure gradient subjected to blowing or suction, the results are quite intriguing.

For example, Fig. 8 shows the plot of $\log(U_\infty)$ vs $\log(\delta)$. Notice that the plot shown exhibits a dependence on the blowing parameter V_0^+, consistent with the results from the similarity analysis and the behavior expected from Eqs. (16–20). As the strength of the blowing parameter increases, the pressure parameter decreases. Inversely, as the blowing parameter decreases the pressure parameter increases, but the flow remains in equilibrium for each particular experiment. In addition, the value Λ changes from 0.136 to about 0.255 and that it is directly affected by the blowing parameter.

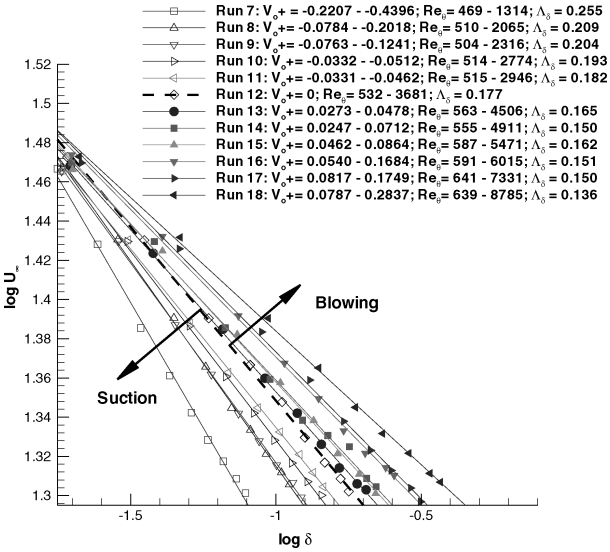

Fig. 8 Pressure parameter based on the boundary-layer thickness $\Lambda_{\delta_{95}}$ represented by the plot of $\log(U_\infty)$ vs $\log(\delta_{95})$.

VI. Conclusions

The mean deficit profiles subjected to suction or blowing in ZPG and APG boundary layers collapse with the freestream velocity, but to different curves depending on the strength of the blowing parameter. This is true as long as the upstream conditions are kept fixed. More importantly, the dependencies on the upstream conditions, pressure gradient, and the blowing parameter are nearly removed from the mean deficit profiles when normalized by the Zagarola/Smits scaling, $U_\infty(\delta_*/\delta)$, and the asymptotic profile for suction is different from that for blowing. Moreover, the classical scaling fails to collapse the profiles, even for ZPG flows. The TH scaling is more efficient in removing the given effects than the classical scaling or the CG scaling. Furthermore, the boundary-layer parameters are affected directly by the blowing parameter. Finally, for the APG data with transpiration, the value of the pressure parameter Λ is a constant for a given experimental test, and its value is directly affected by the blowing parameter $V_0^+ = V_0/U_\infty(\mathrm{d}\delta/\mathrm{d}x)$.

Acknowledgment

The authors are very thankful to Ramona Travis from NASA Stennis Space Center for her continuous support of many of our projects.

References

[1]Simpson, R., Moffat, R. J., and Kays, W. M., "The Turbulent Boundary Layer on a Porous Plate: Experimental Skin Friction with Variable Injection and Suction," *Journal of Heat and Mass Transfer*, Vol. 12, Aug. 1968, pp. 771–789.

[2]Andersen, P. S., Kays, W. M., and Moffat, R. J., "The Turbulent Boundary Layer on a Porous Plate: An Experimental Study of the Fluid Mechanics for Adverse Free-Stream Pressure Gradients," Dept. of Mechanical Engineering, Stanford Univ., Rept. HMT-15, Stanford, CA, May 1972.

[3]Schetz, J. A., and Nerney, B., "Turbulent Boundary Layer with Injection and Surface Roughness," *AIAA Journal*, Vol. 15, No. 9, 1977, pp. 1288–1294.

[4]Clauser, F. H., "Turbulent Boundary Layers in Adverse Pressure Gradients," *Journal of the Aeronautical Sciences*, Vol. 21, No. 2, 1954, pp. 91–108.

[5]Thomas, L. C., and Hasani, S. M., "Equilibrium Boundary Layers—A New Wall/Outer Variable Perspective," *Journal of Fluids Engineering*, Vol. 114, June 1992, pp. 152–154.

[6]Castillo, L., and George, W. K., "Similarity Analysis for Turbulent Boundary Layer with Pressure Gradient: Outer Flow," *AIAA Journal*, Vol. 39, No. 1, 2001, pp. 41–47.

[7]Zagarola, M. V., and Smits, A. J., "Mean-Flow Scaling of Turbulent Pipe Flow," *Journal of Fluid Mechanics*, Vol. 373, 1998, pp. 33–79.

[8]Sucec, J., and Oljaca, M., "Calculation of Turbulent Boundary Layers with Transpiration and Pressure Gradients Effects," *International Journal of Heat and Mass Transfer*, Vol. 38, No. 10, 1995, pp. 2855–2862.

[9]Oljaca, M., and Sucec, J., "Prediction of Transpired Turbulent Boundary Layers with Arbitrary Pressure Gradients," *Transactions of ASME*, Vol. 119, Sept. 1997, pp. 526–532.

[10]Kim, K., Sung, H. J., and Chung, M. K., "Assessment of Local Blowing and Suction in a Turbulent Boundary Layer," *AIAA Journal*, Vol. 40, No. 1, 2002, pp. 175–177.

[11]Antonia, R. A., Zhu, Y., and Sokolov, M., "Effect of Concentrated Wall Suction on a Turbulent Boundary Layer," *Physics of Fluids*, Vol. 7, No. 10, 1995, pp. 2465–2474.

[12]George, W. K., and Castillo, L., "Zero-Pressure Gradient Turbulent Boundary Layer," *Applied Mechanics Reviews*, Vol. 50, No. 11, Pt. 1, 1997, pp. 689–729.

[13]Tennekes, H., and Lumley, J. L., *A First Course in Turbulence*, MIT Press, Cambridge, MA, 1972, pp. 181–186.

[14]Simpson, R. L., "Turbulent Boundary-Layer Separation," *Annual Review of Fluid Mechanics*, Vol. 113, 1989, pp. 205–234.

[15]Wei, T., Klewicki, J. C., and McMurtry, P., "Scaling Properties of the Mean Momentum Balance in Turbulent Wall-Flows," *Journal of Fluid Mechanics* (submitted for publication).

[16]Castillo, L., George, W. K., and Wang, X., "Characterizing Turbulent Boundary Layers Subject to Strong Adverse Pressure Gradient with Eventual Separation," American Society of Mechanical Engineers, Paper 2001-18112, July 2001.

[17]Castillo, L., "Application of Zagarola/Smits Scaling in Turbulent Boundary Layers with Pressure Gradient," *Advances in Fluids Mechanics 3*, edited by M. Rahman and C. A. Brebbia, WIT Press, Southampton, England, U.K., 2000, pp. 275–288.

[18]Seo, J., "Investigation of the Upstream Conditions and Surface Roughness in Turbulent Boundary Layers," Ph.D. Dissertation, Rensselaer Polytechnic Inst., Troy, NY, May 2003.

[19]Castillo, L., and Walker, D. J., "Effects of Upstream Conditions on the Outer Flow of Turbulent Boundary Layers," *AIAA Journal*, Vol. 7, No. 7, 2002, pp. 1292–1299.

[20]Wosnik, M., and George, W. K., "Reconciling the Zagarola/Smits Scaling with the George/Castillo Theory for the Zero Pressure Gradient Turbulent Boundary Layer," AIAA Paper 2000-0911, Jan. 2000.

[21]Townsend, A. A., "Equilibrium Layers and Wall Turbulence," *Journal of Fluid Mechanics*, Vol. 11, No. 1, 1961, pp. 97–120.

H. Atassi
Associate Editor